Int. J. Heat Mass Transfer. Vol. 30, No. 12, pp. 2686–2690, 1987
Printed in Great Britain

0017–9310/87 $3.00 + 0.00

Wall plume at extreme Prandtl numbers

YOGENDRA JOSHI
Department of Mechanical Engineering, Naval Postgraduate School, Monterey, CA 93943-5000, U.S.A.

(*Received* 8 *October* 1986 *and in final form* 10 *June* 1987)

1. INTRODUCTION

NATURAL convection flow arising from a line thermal source at the leading edge of a vertical surface has been the subject of many recent investigations [1–7]. This configuration, also referred to as the wall plume [1], is often a convenient and accurate idealization of many electrical and electronic cooling applications. Such flows are also of importance in studies of boundary layer regimes in transport in enclosures.

None of the studies so far has considered the transport in wall plume at asymptotically large or small Prandtl numbers. Many dielectric fluids used for immersion cooling of electrical and electronic equipment have Prandtl numbers larger than 10. The very low Prandtl numbers, at the other extreme, are characteristic of liquid metals.

Natural convection at extreme Prandtl numbers has been investigated adequately for vertical surfaces. Kuiken [8] obtained solutions to $O(Pr^{-3/2})$ for large Prandtl number natural convection adjacent to a vertical isothermal surface. Matched asymptotic expansions were used to deal with the singular character of the transport equations. The same technique was used by Kuiken [9] to obtain transport to $O(Pr)$ for small Prandtl numbers.

Kuiken and Rotem [10] studied the flow above a line thermal source at asymptotically large and small Pr. Closed form expressions for the velocity and temperature were obtained to $O(Pr^{-1})$ for large Pr. For small Pr, numerical calculations were made up to $O(Pr^{2/3})$.

In the following, an analysis of the wall plume for asymptotically large and small Pr has been carried out. It is shown that the nature of the transport differs significantly from the vertical surface and the line source plume. The asymptotically large Pr condition is studied in Section 2. The other extreme of vanishingly small Pr is considered in Section 3. The various computed quantities are discussed in Section 4. Approximate correlations for transport, applicable for all Pr, have also been obtained.

2. ASYMPTOTIC SOLUTION FOR LARGE *Pr*

Consider the natural convection flow adjacent to a vertical surface with a line heat source along the leading edge. Governing equations with the boundary layer and Boussinesq approximations can be transformed into the following set of non-dimensional equations

$$f''' + \frac{12}{5} f f'' - \frac{4}{5} f'^2 + \phi = 0 \tag{1}$$

$$\phi'' + \frac{12}{5} Pr\,[f\phi]' = 0 \tag{2}$$

where

$$f(\eta) = \psi(x, y)/vc(x), \quad \phi(\eta) = (t - t_\infty)/\Delta T \tag{3}$$

and

$$\eta = yb(x), \quad c(x) = 4xb(x) = 4\left[\frac{g\beta x^3 \Delta T}{4v^2}\right]^{1/4}. \tag{4}$$

In equations (3) and (4), ΔT is the downstream temperature decay along the surface for $Pr = 1$, given by

$$\Delta T = \left[\frac{Q^4}{64\rho^4 v^2 C_p^4 g\beta I^4}\right]^{1/5} x^{-3/5} \tag{5}$$

where

$$I = \int_0^\infty f'\phi \, d\eta = 0.44712$$

is evaluated for $Pr = 1$ and Q is the strength of the line source per unit length.

The boundary conditions for the solution of equations (1) and (2) are

$$f(0) = f'(0) = f'(\infty) = \phi'(0) = \phi(\infty) = 0 \tag{6}$$

and

$$\int_0^\infty f'\phi \, d\eta = I. \tag{7}$$

Note that this formulation of boundary conditions differs from ref. [3] in that $\phi(0) \neq 1$ except for $Pr = 1$. This results from a different choice of ΔT in equation (5), that is now independent of Pr.

For $Pr \gg 1$, the following scaled quantities are introduced in the inner region:

$$\bar{\xi} = Pr^{2/5}\eta, \quad \bar{F}(\bar{\xi}) = Pr^{3/5} f(\eta) \text{ and } \bar{\Phi}(\bar{\xi}) = Pr^{-3/5}\phi(\eta). \tag{8}$$

Using equation (8), equations (1) and (2) are rewritten

$$\bar{F}''' + \frac{1}{Pr}\left[\frac{12}{5}\bar{F}\bar{F}'' - \frac{4}{5}\bar{F}'^2\right] + \bar{\Phi} = 0 \tag{9}$$

$$\bar{\Phi}'' + \frac{12}{5}[\bar{F}\bar{\Phi}]' = 0. \tag{10}$$

Some of the boundary conditions, in addition to equation (7), are

$$\bar{F}(0) = \bar{F}'(0) = \bar{\Phi}'(0) = 0. \tag{11}$$

The remaining conditions are to be found through matching with the outer flow.

The appropriate transformations for the outer region become

$$\tilde{\xi} = Pr^{-1/10}\eta \quad \text{and } \tilde{F}(\tilde{\xi}) = Pr^{1/10} f(\eta). \tag{12}$$

Equation (1) then becomes

$$\tilde{F}''' + \frac{12}{5}\tilde{F}\tilde{F}'' - \frac{4}{5}\tilde{F}'^2 = 0 \tag{13}$$

with the boundary condition

$$\tilde{F}'(\infty) = 0. \tag{14}$$

The remaining boundary conditions are to be found again through matching.

2.1. *Leading order transport*

The leading order or fundamental inner equations are obtained by setting $Pr = \infty$ in equation (9). These are

$$\bar{F}_0''' + \bar{\Phi}_0 = 0 \tag{15}$$

NOMENCLATURE

C_p specific heat of fluid
f non-dimensional stream function, defined in equation (3)
F transformed stream function for large Prandtl number
g acceleration due to gravity
Pr fluid Prandtl number
Q strength of line source per unit length
t temperature
ΔT downstream temperature decay for $y = 0$ and $Pr = 1$ from equation (5)
u component of velocity parallel to surface
v component of velocity normal to surface
V transformed stream function for small Prandtl number
x downstream distance from the heat source
y normal distance from the heat source.

Greek symbols
α thermal diffusivity
β coefficient of thermal expansion
ζ stretched horizontal coordinate for small Pr
η non-dimensional horizontal coordinate given in equation (4)
θ non-dimensional temperature for small Pr
ν kinematic viscosity
ξ stretched horizontal coordinate for large Pr
ρ density
ϕ non-dimensional temperature defined in equation (3)
Φ non-dimensional temperature for large Pr
ψ stream function.

Subscripts
∞ ambient
c composite.

Superscripts
- function or variable in the inner region
~ function or variable in the outer region.

$$\Phi_0'' + \frac{12}{5}[\bar{F}_0\Phi_0]' = 0. \tag{16}$$

The zero order outer transport is governed by

$$\tilde{F}_0''' + \frac{12}{5}\tilde{F}_0\tilde{F}_0'' - \frac{4}{5}\tilde{F}_0'^2 = 0. \tag{17}$$

The additional boundary conditions needed for the solution of equations (15)–(17) are obtained next. The matching condition requires [11]

$$\lim_{\xi\to\infty}\bar{F}(\xi) = Pr^{1/2}\lim_{\tilde{\xi}\to 0}\tilde{F}(\tilde{\xi}). \tag{18}$$

This results in

$$\frac{d^2\bar{F}_0}{d\xi^2}(\infty) = \tilde{F}_0(0) = 0 \quad \text{and} \quad \frac{d\bar{F}_0}{d\xi}(0) = \frac{d\tilde{F}_0}{d\tilde{\xi}}(\infty). \tag{19}$$

Similarly, the matching of temperature yields

$$\Phi(\infty) = 0. \tag{20}$$

Equations (15) and (16) can now be integrated subject to the boundary conditions given in equations (11), (19) and (7). Equation (17) is next solved subject to conditions in equations (19) and (14).

2.2. *First order transport*

In many applications, the fluid Prandtl number is only moderately large. This is true of many commonly used liquids, such as water and some dielectric fluids. To extend the accuracy of the present computations to such fluids, the first order corrections to the transport have also been obtained.

The inner and outer expansions to first order are

$$\bar{F}(\xi) = \bar{F}_0(\xi) + Pr^{-1/2}\bar{F}_1(\xi) \tag{21}$$

$$\Phi(\xi) = \Phi_0(\xi) + Pr^{-1/2}\Phi_1(\xi) \tag{22}$$

and

$$\tilde{F}(\tilde{\xi}) = \tilde{F}_0(\tilde{\xi}) + Pr^{-1/2}\tilde{F}_1(\tilde{\xi}). \tag{23}$$

Substituting these in equations (9), (10) and (13) and collecting terms of the order $Pr^{-1/2}$

$$\bar{F}_1''' + \Phi_1 = 0 \tag{24}$$

$$\Phi_1'' + \frac{12}{5}[\bar{F}_0\Phi_1' + \bar{F}_1\Phi_0' + \bar{F}_0'\Phi_1 + \bar{F}_1'\Phi_0] = 0 \tag{25}$$

and

$$\tilde{F}_1''' + \frac{12}{5}(\tilde{F}_0\tilde{F}_1'' + \tilde{F}_1\tilde{F}_0'') - \frac{8}{5}\tilde{F}_0'\tilde{F}_1' = 0. \tag{26}$$

The boundary conditions are

$$\frac{d^2\tilde{F}_0}{d\tilde{\xi}^2}(0) = \frac{d^2\bar{F}_1}{d\xi^2}(\infty) \quad \text{and} \quad \tilde{F}_1(0) = \lim_{\tilde{\xi}\to\infty}\left(\tilde{F}_0(\tilde{\xi}) - \tilde{\xi}\frac{d\tilde{F}_0}{d\tilde{\xi}}(\xi)\right) \tag{27}$$

and

$$\frac{d\tilde{F}_1(0)}{d\tilde{\xi}}(0) = \lim_{\xi\to\infty}\left[\frac{d\bar{F}_1}{d\xi}(\xi) - \xi\frac{d^2\bar{F}_1}{d\xi^2}(\xi)\right]. \tag{28}$$

Equations (24) and (25) can now be integrated subject to conditions given by equations (11), (27) and the following requirement on the energy integral:

$$\int_0^\infty (\bar{F}_1'\Phi_0 + \bar{F}_0'\Phi_1)\,d\xi = 0. \tag{29}$$

Equation (26) is then solved subject to conditions provided in equations (14) and (28).

3. ASYMPTOTIC SOLUTION FOR SMALL PRANDTL NUMBERS

For $Pr \ll 1$, the thermal boundary layer is much thicker than the momentum boundary layer. The viscous effects are now confined within a thin layer adjacent to the surface. Over most of the outer region, the flow is inviscid to the leading order. In this region, the buoyancy and inertia forces balance.

The appropriate transformations for the outer region are

$$\zeta = Pr^{3/5}\eta, \quad \tilde{V}(\zeta) = Pr^{2/5}f(\eta) \quad \text{and} \quad \tilde{\theta}(\zeta) = Pr^{-2/5}\phi(\eta). \tag{30}$$

Using the above transformations, equations (1) and (2) are rewritten in the outer region

$$Pr\,\tilde{V}''' + \frac{12}{5}\tilde{V}\tilde{V}'' - \frac{4}{5}\tilde{V}'^2 + \tilde{\theta} = 0 \tag{31}$$

$$\tilde{\theta}'' + \frac{12}{5}(\tilde{V}\tilde{\theta}' + \tilde{V}'\tilde{\theta}) = 0. \tag{32}$$

Table 1. Computed transport quantities

		$Pr \gg 1$	
$\tilde{F}_0''(0) = 0.9609$	$\tilde{\Phi}_0(0) = 0.7016$	$\tilde{F}_1''(0) = -0.2424$	$\tilde{\Phi}_1(0) = 0.2659$
$\tilde{F}_0(0) = 0$	$\tilde{F}_0'(0) = 0.7646$	$\tilde{F}_0'(0) = -0.7943$	$\tilde{F}_0(\infty) = 0.6136$
$\tilde{F}_1(0) = -0.4541$	$\tilde{F}_1'(0) = 0.6166$	$\tilde{F}_1''(0) = -0.5035$	$\tilde{F}_1(\infty) = 5.8136 \times 10^{-2}$
		$Pr \ll 1$	
$\tilde{V}_0(0) = 0$	$\tilde{V}_0'(0) = 0$	$\tilde{V}_0''(0) = 1.4222$	$\tilde{\theta}_0(0) = 0.9577$
$\tilde{V}_0'(0) = 1.0941$	$\tilde{\theta}_0(0) = 0.9577$	$\tilde{V}_0(\infty) = 0.6533$	

The imposed boundary conditions are

$$\tilde{V}'(\infty) = \tilde{\theta}(\infty) = 0. \tag{33}$$

The inner layer transformations are

$$\zeta = Pr^{1/10}\eta, \quad \tilde{V}(\zeta) = Pr^{-1/10} f(\eta) \text{ and } \tilde{\theta}(\zeta) = Pr^{-2/5}\phi(\eta). \tag{34}$$

Equations (1) and (2) are then rewritten for the inner region

$$\tilde{V}''' + \frac{12}{5}\tilde{V}\tilde{V}'' - \frac{4}{5}\tilde{V}'^2 + \tilde{\theta} = 0 \tag{35}$$

$$\tilde{\theta}'' + \frac{12}{5}Pr\,(\tilde{V}\tilde{\theta}' + \tilde{V}'\tilde{\theta}) = 0. \tag{36}$$

The boundary conditions known at this stage are

$$\tilde{V}(0) = \tilde{V}'(0) = \tilde{\theta}'(0) = 0. \tag{37}$$

It is noted that the second condition in equation (37) differs from those for the line plume [10]. The leading order outer solutions are next obtained by setting $Pr = 0$ in equation (31). In order to achieve matching with the inner solution, expansions in powers of ζ are required for $\tilde{V}_0(\zeta)$ and $\tilde{\theta}_0(\zeta)$ near $\zeta = 0$. These are

$$\tilde{V}_0(\zeta) = A_0\zeta + O(\zeta^{5/3}) \tag{38}$$

$$\tilde{\theta}_0(\zeta) = 4\frac{A_0^2}{5} + O(\zeta^2) \tag{39}$$

where A_0 is to be determined numerically.

Matching with the inner solution and allowing the integral in equation (12) to have a finite contribution, results in the following additional boundary conditions:

$$\tilde{V}_0(0) = 0 \quad \text{and} \quad \int_0^\infty \tilde{V}_0'\tilde{\theta}_0\,d\zeta = I. \tag{40}$$

Equations (31) and (32) can now be solved subject to conditions in equations (33) and (40). This yields $A_0 = 1.0941$.

By setting $Pr = 0$ in equation (36) and using equation (37), it is clear that the inner region is isothermal to the leading order. Matching of temperature and velocity further requires

$$\tilde{\theta}_0 = \frac{4A_0^2}{5} \quad \text{and} \quad \tilde{V}_0'(\infty) = A_0. \tag{41}$$

Equation (35) can now be solved for $\tilde{V}_0(\zeta)$ subject to conditions provided by equations (37) and (41).

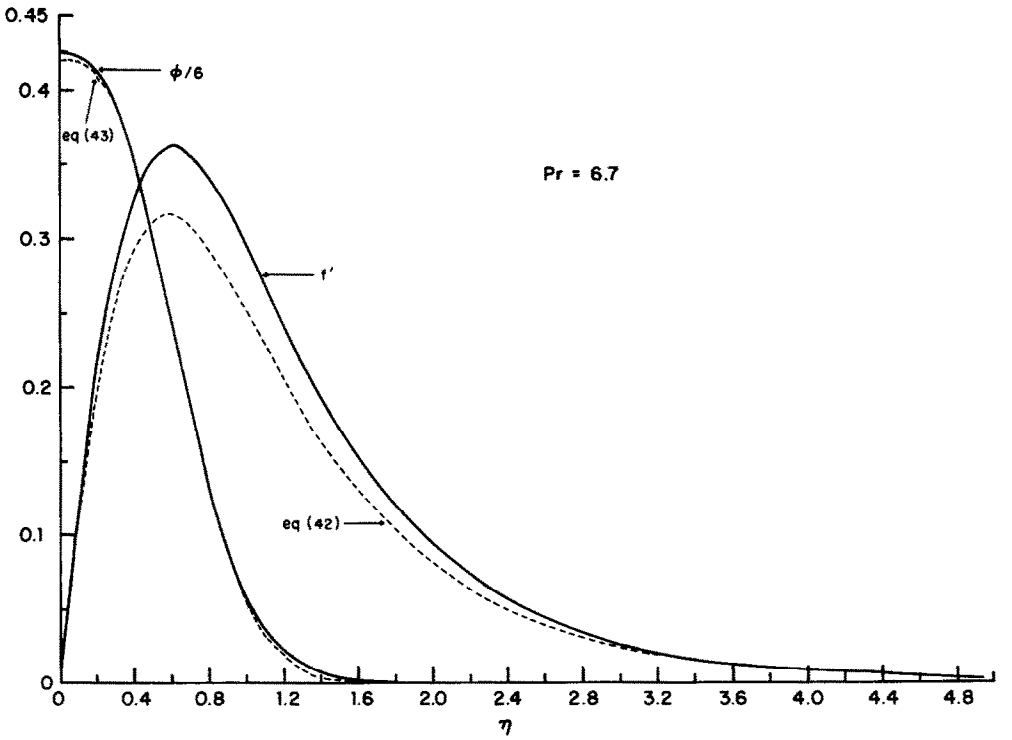

FIG. 1. Comparison of the two-term composite velocity and temperature functions with numerical solution of the boundary layer equations, for $Pr = 6.7$.

4. COMPUTATIONS AND RESULTS

The non-dimensional velocity and temperature functions in Sections 2 and 3 have been computed. These are available in ref. [12]. The important transport quantities are collected in Table 1 both for $Pr \gg 1$ and $Pr \ll 1$.

The two-term composite tangential velocity function is obtained as (see ref. [11])

$$f'_c = \frac{Pr^{-1/5}[\bar{F}'_0 + Pr^{-1/2}\bar{F}'_1][\bar{F}'_0 + Pr^{-1/2}\bar{F}'_1]}{\{\bar{F}'_0(0) + \xi\bar{F}''_0(0) + Pr^{-1/2}\bar{F}'_0(0)\}}. \quad (42)$$

Since the outer region is isothermal, the composite temperature profile is simply

$$\phi_c = Pr^{3/5}(\bar{\Phi}_0(\xi) + Pr^{-1/2}\bar{\Phi}_1(\xi)). \quad (43)$$

The composite velocity and temperature equations (42) and (43) are seen in Fig. 1, for $Pr = 6.7$. Also shown for comparison are the computed profiles from integrating equations (1) and (2). Even though the Prandtl number is only moderately large, the agreement is good. A similar comparison of the small Prandtl number, one-term inner and outer functions, with the numerical solution of equations (1) and (2) is seen in Fig. 2 for $Pr = 0.01$. Again, the numerical solutions tend to approach the asymptotic profiles.

4.1. *Approximate transport correlations for all Pr*

The results of the analysis in Sections 2 and 3 are next used to obtain approximate expressions for various transport quantities, valid for all Pr. Such correlations are obtained using the technique proposed by Churchill and Usagi [13]. This technique utilizes a suitable combination of the two asymptotic limits of a function, to construct a universal correlation.

The resulting expression for the non-dimensional surface temperature is

$$\phi(0) = 0.7016Pr^{3/5}\left[1 + \left(\frac{4.7403}{Pr}\right)^{4/5}\right]^{1/4}. \quad (44)$$

It is found [12] that for extreme values of Pr, the limiting expressions obtained in Sections 2 and 3 are more accurate than equation (44). However, equation (44) provides estimates of $\phi(0)$ for all Pr, with a maximum error of about 2%.

Approximate expressions for the non-dimensional surface shear stress and the mass flow rate are constructed in an identical manner. There are

$$f''(0) = ((0.9609Pr^{1/5})^{-4.6} + (1.4222Pr^{3/10})^{-4.6})^{-0.217} \quad (45)$$

and

$$f(\infty) = ((0.6533Pr^{-2/5})^{3.4} + (0.6136Pr^{-1/10})^{3.4})^{0.294}. \quad (46)$$

The use of equations (44)–(46) allows the evaluation of various transport quantities without the complete integration of the governing equations, for any Pr.

5. CONCLUSIONS

Transport in a wall plume at asymptotically large and small Prandtl numbers exhibits differences from vertical surfaces and the line plume. At very high Prandtl numbers, this results from a different set of scaling requirements. Unlike the vertical surface, the wall plume requires conservation of the total convected energy. Also, unlike the line plume, the tangential velocity now must vanish at the surface. For very low Pr, the scaling requirements are identical to those in the line plume. The difference in transport now results purely from changed boundary conditions at the surface. The use of the matched asymptotic expansions technique allows examination of the entire flow and transport region. Transport quantities of practical importance have been obtained in the form of correlations, where Pr occurs as a multiplicative function.

Acknowledgements—The author acknowledges support for this work through the Naval Postgraduate School Foundation Research Program. The final manuscript was prepared by Mrs Karen Brylewski.

REFERENCES

1. V. D. Zimin and Y. N. Lyakhov, Convective wall plume, *J. Appl. Mech. Tech. Phys.* **11**, 159 (1970). Translated from Russian, January 1973.

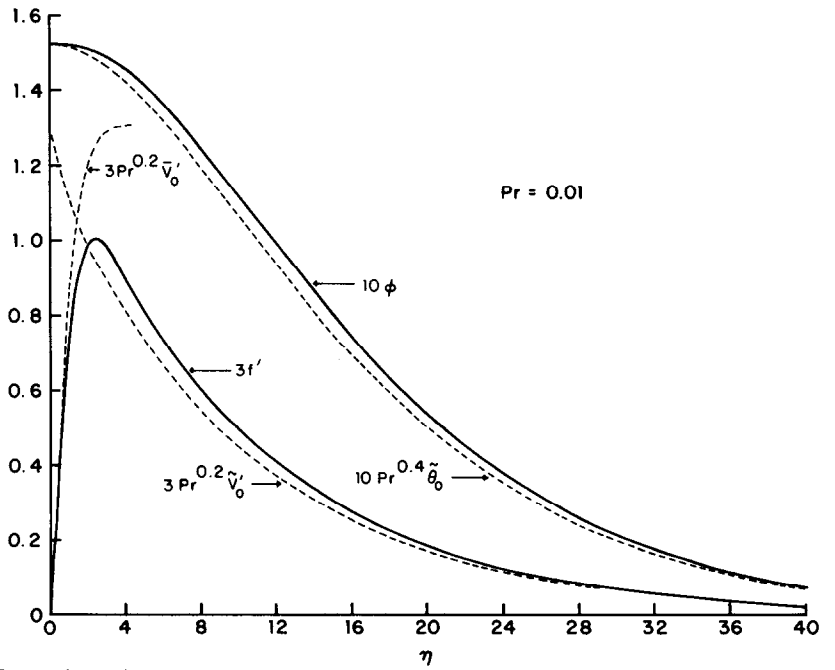

FIG. 2. Comparison of the one-term inner and outer functions with the numerical solution of the boundary layer equations, for $Pr = 0.01$.

2. J. A. Liburdy and G. M. Faeth, Theory of steady laminar thermal plume along a vertical adiabatic wall, *Lett. Heat Mass Transfer* **2**, 407–418 (1975).
3. Y. Jaluria and B. Gebhart, Buoyancy-induced flow arising from a line thermal source on an adiabatic vertical surface, *Int. J. Heat Mass Transfer* **20**, 153–157 (1977).
4. J. J. Grella and G. M. Faeth, Measurements in a two dimensional thermal plume along a vertical adiabatic wall, *J. Fluid Mech.* **71**, 701 (1975).
5. N. Afzal, Convective wall plume: higher order analysis, *Int. J. Heat Mass Transfer* **23**, 505–513 (1980).
6. Y. Jaluria, Mixed convection in a wall plume, *Comput. Fluids* **10**, 95–105 (1982).
7. R. Krishnamurthy and B. Gebhart, Mixed convection in a wall plume, *Int. J. Heat Mass Transfer* **27**, 1679–1689 (1984).
8. H. K. Kuiken, An asymptotic solution for large Prandtl number free convection, *J. Engng Math.* **2**, 355–371 (1968).
9. H. K. Kuiken, Free convection at low Prandtl numbers, *J. Fluid Mech.* **37**, 785–798 (1969).
10. H. K. Kuiken and Z. Rotem, Asymptotic solution for plume at very large and small Prandtl numbers, *J. Fluid Mech.* **45**, 585–600 (1971).
11. M. Van Dyke, *Perturbation Methods in Fluid Mechanics* (Annotated Edition), Chap. 7. Parabolic Press, Stanford, California (1975).
12. Y. Joshi, Transport in a wall plume at very large and very small values of the Prandtl number, U.S. Naval Postgraduate School Report NPS 69-87-004 (1987).
13. S. W. Churchill and R. Usagi, A general expression for the correlation of rates of transfer and other phenomena, *A.I.Ch.E. Jl* **18**, 1121–1128 (1972).

Int. J. Heat Mass Transfer. Vol. 30, No. 12, pp. 2690–2694, 1987
Printed in Great Britain

0017–9310/87 $3.00 + 0.00

A fixed grid numerical methodology for phase change problems involving a moving heat source

C. PRAKASH, M. SAMONDS and A. K. SINGHAL
CHAM of North America, Incorporated, 1525-A Sparkman Drive, Huntsville, AL 35816, U.S.A.

(*Received* 3 *November* 1986 *and in final form* 9 *June* 1987)

INTRODUCTION

MANY PROBLEMS arise in engineering in which heat transfer is accompanied by melting and solidification (phase change). The situation is particularly common in materials processing, e.g. welding, casting, heat treatment, crystal growth, etc. The work described in this note has been motivated by application to TIG (tungsten inert gas) or GTA (gas tungsten arc) welding processes [1]. The situation is described schematically in Fig. 1. A source of heat (arc) moves laterally over the surface of a plate to be welded. Due to intense heating, the material under the arc melts and, as the arc moves away, the material resolidifies resulting in a welded joint.

In this technical note a fixed grid numerical methodology is presented for solving phase change problems involving a moving heat source. The spirit of the paper is to emphasize only on the methodology and illustrate the procedure via a two-dimensional example; the solution for a complete three-dimensional TIG problem including the flow in the melt due to buoyancy, surface tension and electromagnetic forces, etc. is the subject of a separate paper [2] targeted for the material sciences community.

Viewed in the laboratory coordinates, the arc problem described in Fig. 1 is inherently unsteady. However, if one works with a coordinate system fixed to the arc, then the problem becomes steady, assuming the plate length to be infinite in the direction of arc motion. This note deals with such a steady state problem only; thus the arc and the melt under it are fixed in space while material enters and leaves the computational domain.

THE PROPOSED PHASE CHANGE METHODOLOGY

There are two approaches to solving phase change problems. The classical problem requires tracking of the phase change front by the satisfaction of the Stefan condition. This is often implemented computationally by deforming grid techniques. For steady state problems, this procedure would involve adjusting the grid 'iteratively' until the appropriate interface conditions have been satisfied.

Alternatively, the 'weak' or integral formulation of the Stefan problem leads to enthalpy methods which employ fixed grids. The technique proposed here falls into this second class. An important attribute of this method is its ease of implementation. The scheme has evolved from the recent work of Voller *et al.* [3, 4] and the concurrent work of Voller and Prakash [5].

The basic idea is to represent the total enthalpy as a sum of sensible and latent heats, i.e.

$$\underset{\text{total enthalpy}}{H} = \underset{\text{sensible enthalpy}}{h} + \underset{\text{latent heat}}{\Delta H} \tag{1}$$

where

$$h = c_p T \tag{2}$$

c_p being the specific heat and T the temperature. The latent heat, ΔH, is constrained by the limits

$$0 \leqslant \Delta H \leqslant L \tag{3}$$

where L represents the total latent heat of fusion. Thus, at any point, the value of ΔH has the following physical interpretation:

$$\text{liquid fraction} = \frac{\Delta H}{L} \tag{4}$$

$$\text{solid fraction} = 1 - \frac{\Delta H}{L}. \tag{5}$$

The energy conservation equation for steady situation can be written as

$$\nabla \cdot (\rho \mathbf{u} H) = \nabla \cdot \left(\frac{k}{c_p} \nabla h \right) \tag{6}$$

where ρ represents the density, $\mathbf{u}$ the material velocity and k and c_p are the thermal conductivity and specific heat of the material, respectively. Substituting equation (1) into equa-